

## Steady-state and transient electron transport within bulk ternary nitride semiconductors including GaInN, AlGaN and AlInN using a three-valley Monte Carlo method

M. Rezaee Rokn-Abadi

Department of Physics, Ferdowsi University of Mashhad, Mashhad, Iran

roknabad@um.ac.ir

### Abstract

An ensemble Monte Carlo simulation is used to compare bulk electron transport in wurtzite phase GaInN, AlGaN and AlInN materials. Electronic states within the conduction band valleys at the  $\Gamma$ , U and K are represented by non-parabolic ellipsoidal valleys centered on important symmetry points of the Brillouin zone. For all materials it is found that electron velocity overshoot only occurs when the electric field is increased to a value above a certain critical field, unique to each material. This critical field is strongly dependent on the material parameters. Transient velocity overshoot has also been simulated with the sudden application of fields up to  $\sim 5 \times 10^7 \text{ Vm}^{-1}$ , appropriate to the gate-drain fields expected within an operational field effect transistor. The electron drift velocity relaxes to the saturation value of  $\sim 1.5 \times 10^5 \text{ ms}^{-1}$  with in 4 ps for all crystal structures. The steady-state and transient velocity overshoot characteristics are in fair agreement with other recent calculations.

**Keywords:** Brillouin zone, gate-drain, transient, critical field, drift velocity, semiconductor

### Introduction

GaInN quantum wells represent a key constituent in the active regions of blue diode lasers and LEDs. This technological significance justifies the quest for a thorough understanding of the bulk properties of wurtzite GaInN alloys (Besikci *et al.*, 2000). However there is still considerable disagreement over such fundamental parameters as the bowing of the energy gap. A phase decomposition of the GaInN quantum wells employed in blue and green LEDs is believed to occur (Fischetti & Laux, 1991). Nearly pure InN quantum dots are formed which act as efficient radiative recombination centers. Since it is not yet clear whether this phase segregation has been completely avoided in thicker layers of GaInN interpretation of the reported bowing parameters requires great care. AlGaN is often used as the barrier material for nitride electronic and optoelectronic devices. Initial studies of the compositional dependence of the energy gap reported downward, upward and negligible bowing. Subsequent early PL and absorption measurements found a bowing parameter of 1 eV, which continues to be widely used in band structure calculations even though a number of more recent investigations question the conclusions of the early work. Several studies found negligible bowing and it has been suggested that the other values resulted from an incomplete relaxation of strain in the AlGaIn thin films (Foutz *et al.*, 1997).

This statement is supported to some extent by a large bowing parameter of 1.78 eV reported for highly strained layers grown on SiC. Other workers quite recently calculated and measured smaller bowing parameters  $\sim 0.25$ -0.6 eV depending on the measurement method and assumed binary end points (Ghani *et al.*, 2003). AlInN is drawing attention because it can be lattice matched to GaN. The first experimental study observed such a strong bowing that the band gap for the lattice-matched

composition was found to be smaller than that of GaN. Furthermore, the standard quadratic expression did not fit the compositional variation of the band gap very well.

Izuka *et al.* (1990) subsequently presented results for InN-rich and AlN-rich AlInN, respectively which indicated somewhat weaker bowing. Bhuiyam *et al.* (2003) gave a cubic expression for the energy gap based on results over the entire range of compositions (Brennan *et al.*, 1983). A similarly large bowing was observed by Izuka *et al.* (1990). On the theoretical side, a first-principles calculation for zincblende AlInN yielded a bowing parameter of 2.53 eV which was assumed to be equal to that in the wurtzite alloy. These ternary compounds have received much attention over the past years because of several new applications, including blue light-emitting diodes (LEDs), blue laser diodes (LDs) and high-power microwave transistors (Bhappkar *et al.*, 1997). For the above stated reasons these ternary compounds are of great interest for power FET and optoelectronic device structures. To clarify the expected performance of these materials, transport as well as device studies are critical. Thus, it is the purpose of this paper to compare steady-state and transient velocity overshoot in these ternary compounds material using an ensemble Monte Carlo study. This paper is organized as follows. Details of the employed simulation model are presented in section 2 and the results of steady-state and transient electron transport properties are interpreted in section 3. Simulation model

Our ensemble Monte Carlo simulations of electron transport in ternary compounds of GaInN, AlGaIn and AlInN are similar to those of Arabshahi *et al.* (2008). As indicated earlier, a three-valley model for the conduction band is employed. In order to calculate the electron drift velocity for large electric fields, consideration of conduction band satellite valleys is necessary. The first-

principles band structure of wurtzite band structure predicts a direct band gap located at the  $\Gamma$  point and lowest energy conduction band satellite valleys at the U point and at the K point. In our Monte Carlo simulation, the  $\Gamma$  valley, the six equivalent U valleys, the two equivalent K valleys, are represented by ellipsoidal, non-parabolic dispersion relationships of the following form (Jacoboni *et al.*, 1989).

$$E(k)[1 + \alpha_i E(k)] = \frac{\hbar^2 k^2}{2m^*} \quad (1)$$

Where  $m^*$  is effective mass at the band edge and  $\alpha_i$  is the non-parabolicity coefficient of the  $i$ th valley given by Kane model (Jacoboni *et al.*, 1983) as

$$\alpha_i = \frac{1}{E_g} \left[ 1 - \frac{2m^*}{m_0} \right] \left[ 1 - \frac{E_g \Delta}{3(E_g + \Delta)(E_g + 2\Delta/3)} \right] \quad (2)$$

Where  $E_g$  is the band-gap energy and  $\Delta$  is the spin-orbit splitting. We assume that all donors are ionized and that the free-electron concentration is equal to the dopant concentration. For each simulation, the motion of 10,000 electron particles are examined, the temperature being set to 300 K, and the doping concentration being set to  $10^{17} \text{ cm}^{-3}$ . In the case of the ellipsoidal, non-parabolic conduction valley model, the usual Herring-Vogt transformation matrices are used to map carrier momenta into spherical valleys when particles are drifted or scattered. Electrons in bulk material suffer intravalley scattering by polar optical, non-polar optical and acoustic phonons scattering, intervalley phonons, and ionized impurity scattering.

Acoustic scattering is assumed elastic and the absorption and emission rates are combined under the equipartition approximation, which is valid for lattice temperatures above 77 K. Elastic ionized impurity scattering is described using the screened coulomb potential of the Brooks-Herring model. Band edge energies, effective masses and non-parabolicities are derived from empirical pseudopotential calculations.

In the case of ternary compounds the alloy scattering have also been included. Alloy scattering refers to the scattering due to the random distribution of the component atoms of the alloy among the available lattice sites. Jacoboni *et al.* (1989) assumed that the alloy crystal potential can be described as a perfectly periodic potential which is then perturbed by the local deviations from this potential, due to the disordering effects in the alloy. Using the Harrison model, the scattering rate due to the chemical disorder in a ternary alloy of electrons in a non-parabolic band is given by

$$R_{\text{alloy}}(k) = \frac{4\sqrt{2}\pi n^{*3/2} r^6}{9\hbar^4} \cdot \frac{x(1-x)\Delta U^2}{\Omega^2} \gamma^{1/2}(E)(1+2\alpha E) \quad (3)$$

Where  $x$  denotes the molar fraction of one of the binary components of the alloy  $\Omega$  is the volume of the primitive cell and  $\Delta U$  is the spherical scattering potential.

Research article

©Indian Society for Education and Environment (ISee)

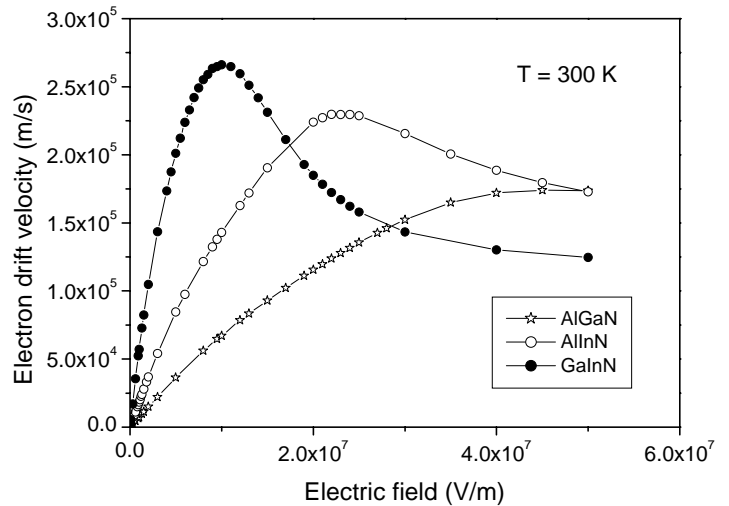
"Wurtzite GaInN alloys"

<http://www.indjst.org>

M. Rezaee

Indian J.Sci.Technol.

Fig. 1. Calculated electron drift velocity in AlGaIn, GaInN & AlInN as function of applied electric field at room temperature



**Results of simulation**

The bulk ternary nitride velocity-field characteristics, predicted by our model are shown in Fig. 1. For all cases, the temperature is 300 K and the donor concentration is  $10^{22} \text{ m}^{-3}$ . We see that each compound exhibits a peak in its velocity-field characteristic. The peak drift velocity for GaInN is around  $2.8 \times 10^5 \text{ ms}^{-1}$  while those for AlInN and AlGaIn are about  $2.4 \times 10^5 \text{ ms}^{-1}$  and  $1.6 \times 10^5 \text{ ms}^{-1}$ , respectively. At higher electric fields the drift velocity decreases, eventually saturating at around  $1.6 \times 10^5 \text{ ms}^{-1}$  and  $1.2 \times 10^5 \text{ ms}^{-1}$  for AlGaIn, AlInN and GaInN respectively.

The calculated drift velocities apparent from Fig. 1 are fractionally lower than those calculated by Wang *et al.* (1997) who assumed an effective mass in the upper valleys equal to the free electron mass. The threshold field for the onset of significant scattering into satellite conduction band valleys is a function of the intervalley separation and the density of electronic states in the

Fig. 2. Average electron kinetic energy as a function of applied electric field in bulk AlGaIn, GaInN & AlInN using the non-parabolic band model

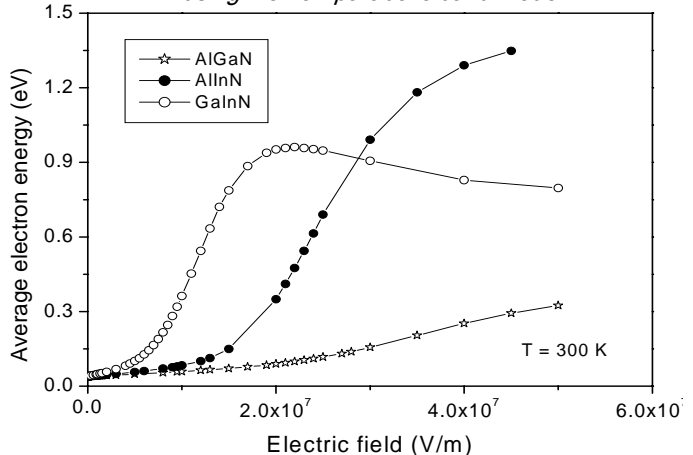
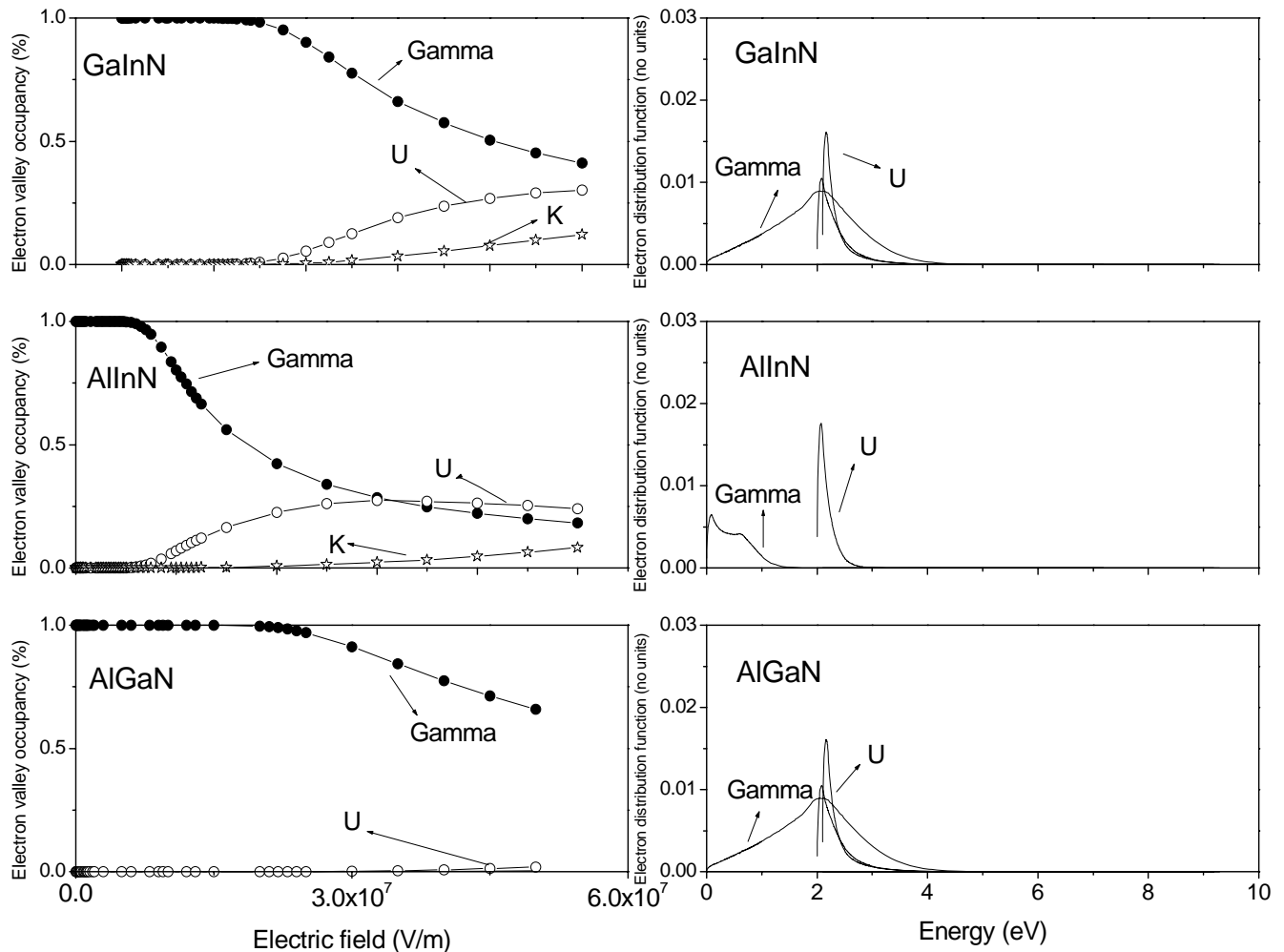


Fig. 3. Comparison of the valley occupancies & their normalized electron distribution function in wurtzite GaInN, AlInN & AlGaN with GaN for  $\Gamma$ , U & K valleys at room temperature.



satellite valleys.

The average carrier kinetic energy as a function of electric field is shown in Fig. 2. The curves have the S shape typical of III-V compounds which is a consequence of intervalley transfer. At high fields, the curve for AlInN suggests that the average electron energy is higher than for two other structures. This difference can be understood by considering the lower  $\Gamma$  valley electron effective mass and a lower electron occupancy in this valley as a function of field as it can be seen from Fig. 3.

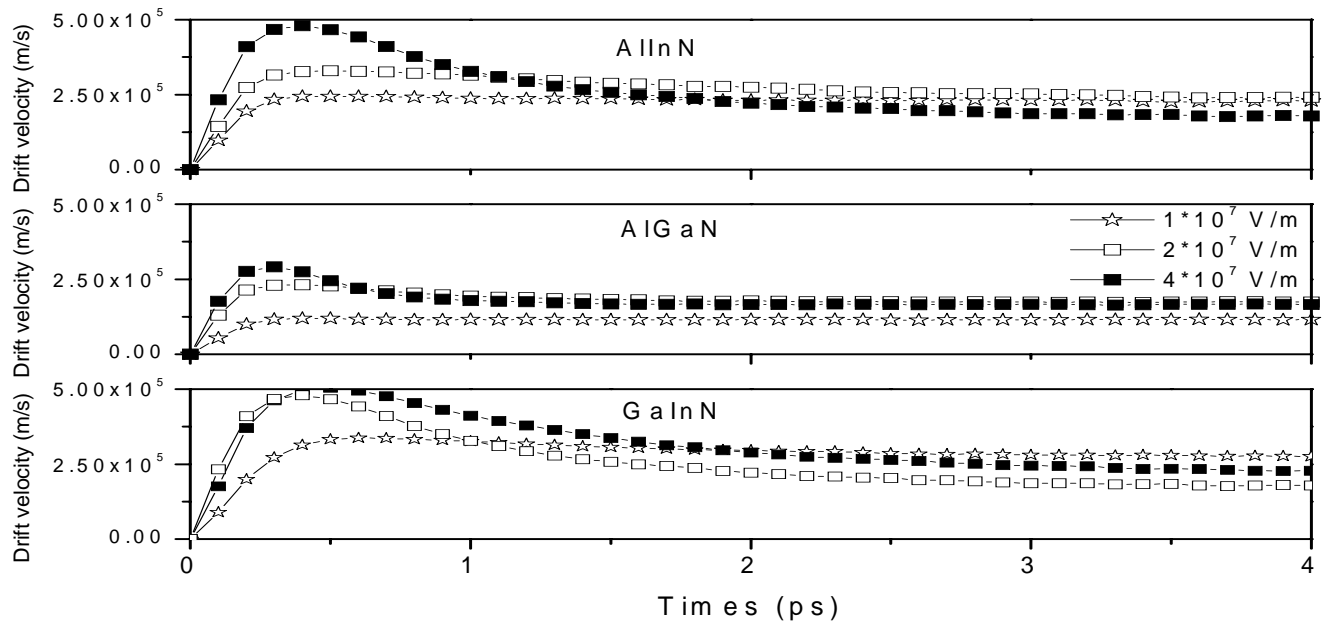
The valley occupancies for the  $\Gamma$ , U and K valleys are illustrated in Fig. 3 and show that the inclusion of the satellite valleys in the simulation is important. Significant intervalley scattering into the satellite valleys occurs for fields above the threshold field for each material. This is important because electrons which are near a valley minimum have small kinetic energies and are therefore strongly scattered. It is apparent that intervalley transfer is substantially larger in GaInN over the range of applied electric fields shown, due to the combined effect of a lower  $\Gamma$  effective mass, lower satellite valley separation

energy and slightly lower phonon scattering rate within the  $\Gamma$  valley.

Fig. 3 also shows the electron energy distribution functions for various valleys at an electric field of  $5 \times 10^7 \text{ Vm}^{-1}$ , which is in the saturation regime. These distribution functions show similar features to those described previously for GaN and can be interpreted in terms of each material's band structure. We notice that the electron populations in the  $\Gamma$  valley of InGaN and AlGaN increase until an energy of around 2 eV and after that decrease due to scattering to the satellite valleys. The behaviour of AlN is quite different. This is because of the relatively small  $\Gamma$ -satellite valley energy separation and the larger  $\Gamma$  effective mass of AlGaN. At the field corresponding to the peak velocity in AlInN we find, occupancies of 14% and 2% for the U and K valleys.

We have also examined transient electron transport in bulk GaInN, AlInN and AlGaN. The transient response of electrons in these materials is compared in Fig. 4 for different electric field strengths. Note that the overshoot velocity in GaInN is higher and is more enduring than for

Fig. 4. A comparison of the velocity overshoot effect exhibited by the AlInN, AlGaIn and GaInN semiconductors as calculated by our Monte Carlo simulation. The donor concentration is  $10^{22} \text{ m}^{-3}$  & the temperature is 300 K.



the other materials. When the field is increased to  $4 \times 10^7 \text{ Vm}^{-1}$  the peak velocity in GaInN increases to  $5 \times 10^5 \text{ ms}^{-1}$ . The velocity overshoot effect in AlGaIn is markedly weaker. This is because of the smaller intervalley energy separation, 0.6 eV (versus 1.6 eV in GaInN and 1.9 eV in AlInN) and larger  $\Gamma$  effective mass,  $0.3 m_0$  (versus  $0.2 m_0$  in AlGaIn and  $0.11 m_0$  in AlInN). The smaller satellite energy separation means, the electrons readily transfer to the satellite valleys, resulting in a reduced average electron velocity and the rapid removal of overshoot.

### Conclusion

The computed steady-state and transient electron transport in wurtzite AlGaIn, AlInN and GaInN show that GaInN has superior electron transport properties. The velocity-field characteristics of the materials show similar trends, reflecting the fact that these semiconductors have satellite valley effective densities of states several times greater than the central  $\Gamma$ -valley. We have also shown that GaInN exhibits much more pronounced overshoot effects compared to AlGaIn but at much higher electric fields. Using valley models to describe the electronic band structure, it is found that electron drift velocity relaxes to the saturation value within 3 ps in ternary nitrides crystal structures.

### Acknowledgments

This work is supported by the Ferdowsi University of Mashhad through a contract with Vice President for Research and Technology.

### References

1. Arabshahi H, Khalvati MR and Rezaee Rokn-Abadi M (2008) Monte Carlo modeling of hot electron transport in bulk AlAs, AlGaAs and GaAs at room temperature. *Modern Phys. Lett. B*, 22 (18), 1777-1784.

2. Besikci B, Bakir M and Tanatar U (2000) Hot electron simulation devices. *J. Appl. Phys.* 88(3), 1243-1247.
3. Bhapkar UV and Shur MS (1997) Ensemble Monte Carlo study of electron transport in wurtzite InN. *J. Appl. Phys.* 82, 1649-1654.
4. Bhuiyam S, Senoh M and Mukai T (2003) Comparison of steady state and transient electron. *Appl. Phys. Lett.* 62, 2390-2395.
5. Brennan K, Hess K, Tang JY and lafrate GT (1983) High field electron transport properties. *IEEE Trans. Elec. Dev.* 30, 1750-1755.
6. Fischetti MV and Laux SE (1991) Low field electron mobility in GaN. *IEEE Trans. Elec. Dev.* 38, 650-655.
7. Foutz BE, Eastman LE, Bhapkar UV and Shur M (1997) Full band Monte Carlo simulation of Zincblende GaN MESFET's including realistic impact ionization rates. *Appl. Phys. Lett.* 70, 2849-2854.
8. Ghani B, Hashimoto A and Yamamoto A (2003) High temperature characteristics of AlGaIn/GaN modulation doped field-effect transistors. *J. Appl. Phys.* 94, 2779-2783.
9. Izuka J and Fukuma M (1990) Full-band polar optical phonon scattering analysis and negative differential conductivity in wurtzite GaN. *Solid-State Elec.* 3, 27-33.
10. Jacoboni J and Lugli P (1989) The Monte Carlo method for semiconductor and device simulation. Springer-Verlag.
11. Jacoboni J and Reggiani L (1983) The Monte Carlo simulation of semiconductor and devices. *Rev. Modern Phys.* 55(3), 665-663.
12. Wang R P, Ruden P P, Kolnik J and Brennan K F (1997) Hot transport properties in group III nitrides. *Mat. Res. Soc. Symp. Proc.* 445, 935-941.